Ecology, 86(6), 2005, pp. 1441–1451

ANALYSIS OF SIZE TRAJECTORY DATA USING AN ENERGETIC-BASED GROWTH MODEL

MASAMI FUJIWARA,[1,4] BRUCE E. KENDALL,[2] ROGER M. NISBET,[1] AND WILLIAM A. BENNETT[3]

[1]*Department of Ecology, Evolution, and Marine Biology, University of California, Santa Barbara, California 93106-9610 USA*
[2]*Donald Bren School of Environmental Science and Management, University of California, Santa Barbara, California 93106-5131 USA*
[3]*John Muir Institute of the Environment, Bodega Marine Laboratory, University of California, Davis, California 95616 USA*

Abstract. Individual growth rate of animals is increasingly used as an indicator of ecological stressors. Environmental contaminants often affect physiological processes within individuals, which in turn affect the animal's growth rate. Consequently, there is an increasing need to estimate parameters in physiologically based individual growth models. Here, we present a method for estimating parameters in an energetic-based individual growth model (a dynamic energy budget model). This model is a system of stochastic differential equations in which one of the state variables (the energy reserve) is unobservable. There is no analytical solution to the probability density of size at given age, so we use a numerical nonlinear state–space method to calculate the likelihood. An algorithm to calculate the likelihood is outlined in this paper. This method is general enough to apply to other stochastic differential equation models. We assessed the estimability of parameters in the individual growth model, and analyzed size trajectory data from delta smelt (*Hypomesus transpacificus*). We expect this method to become an important tool in ecological studies as computers become faster, as the models that we deal with become more complex, and as the data that we collect become more detailed.

Key words: *bioenergetics; dynamic energy budget; energy reserves; fluctuating food;* Hypomesus transpacificus; *individual growth model; nonlinear state–space analysis; numerical maximum likelihood; parameter estimation; size trajetory data; stochastic differential equation model.*

INTRODUCTION

Individual growth of many animal species exhibits tremendous plasticity, producing a large amount of individual size variability (e.g., Wikelski et al. 1997, Pfister and Stevens 2002, Gurney et al. 2003). This variability reflects past and current environmental conditions. For example, past environmental conditions can determine genetic variability, producing heterogeneity in the growth rate among individuals that persists throughout their entire life histories. On the other hand, present resource heterogeneity in the environment can produce instantaneous differences in growth rate (Pfister and Peacor 2003), even among genetically identical individuals. Regardless of the causes of growth variability, consequent size variability is an important indicator of population performance because the size of individuals often determines how well the individuals utilize food resources, escape predation pressure, and reproduce (e.g., Caswell 2001: Section 3.2.1). Consequently, understanding variability in individual growth can provide important information that links population processes and the environment (see Rice et al. 1993, Nisbet et al. 2000).

Individual growth is a complex energetic process. Individual length increases only when enough energy from food is available for growth. On the other hand, a lack of food does not always lead to a reduction in length, because organisms can lose body mass without shrinking in length (Kooijman 2000, Nisbet et al. 2000). Energy may also be allocated to storage for future use, producing ''memory'' in growth dynamics. A model that encapsulates these characteristics is a dynamic energy budget model (Kooijman 2000, Nisbet et al. 2000).

Dynamic energy budget (DEB) models are based on energetic pathways such as the one shown in Fig. 1. The energetic pathways depict how ingested food is stored and utilized for growth, reproduction, and maintenance of individuals. There are many studies that fit deterministic DEB models to data on growth and reproduction of individual organisms (e.g., Kooijman 1986, Gurney et al. 1990, Noonburg et al. 1998, Nisbet et al. 2004), and a few that use fitted DEB models to reconstruct the environment experienced by organisms whose growth history is known (van Haren and Kooijman 1993). However, a stochastic version of these models is yet to be explored beyond theoretical studies (e.g., Muller and Nisbet 2000, Fujiwara et al. 2004).

Manuscript received 31 August 2004; accepted 21 October 2004; final version received 11 November 2004. Corresponding Editor: L. Stone.

[4] E-mail: fujiwara@lifesci.ucsb.edu

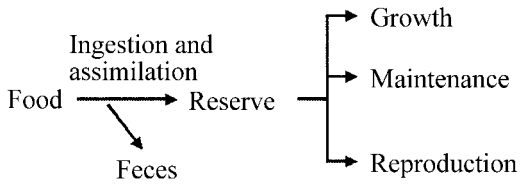

FIG. 1. Energy flow within individuals (see Kooijman [2000] for details). The feeding rate is assumed to be proportional to the surface area of individuals. A fixed fraction of energy flux coming out of the reserve is used for maintenance and growth, and the rest is used for reproduction, including development of reproductive organs.

Here we present an analysis of individual size trajectory data to study individual growth dynamics in a fluctuating resource environment. We consider longitudinal data in which the size of the same individuals is measured repeatedly over time. Longitudinal size data are advantageous because they provide information on how changes in individual size vary among individuals and over time (see Diggle et al. 2002). The collection of size trajectory data is becoming increasingly more common in ecological studies. In the laboratory, the size of individuals is followed to investigate the influence of toxicity (e.g., Kooijman and Bedaux 1996) and other environmental factors (e.g., Cox and Coutant 1981, Rogers and Westin 1981) on growth rate. In the field, the size of marked individuals is often followed over time to investigate the origin of size variability among individuals (Pfister and Stevens 2002). In addition to these direct measurements, the size history of teleost fish can be inferred using the daily rings laid down in otoliths (Campana and Neilson 1985).

We fit an energetic-based individual growth model to size trajectory data using a nonlinear state–space model technique. This technique is commonly called particle filtering or sequential Monte Carlo method in statistics literature (see Gordon et al. 1993, Doucet et al. 2001, de Valpine 2004). It allows the inclusion of unobservable state variables, a common feature in many ecological models, when estimating parameters. As an example, we apply the method to data on the delta smelt (*Hypomesus transpacificus*), a federally listed threatened species of fish (U.S. Department of Interior 1994) that is endemic to San Francisco Estuary, California, USA (Moyle et al. 1992, Sweetnam 1999, W. A. Bennett, *unpublished manuscript*). The statistical method outlined here is general enough to apply to estimating parameters in other stochastic differential equation models when longitudinal data are available. Therefore, the section describing the method will also be beneficial to readers with interest in the parameter estimation procedure, but not necessarily in the study of individual growth.

The paper has four main parts. First, we will present a growth model that describes how individual growth changes with individual size and available food. Second, we will demonstrate a method to fit the model to the size trajectory data using a nonlinear state–space method. Then we investigate the estimability of parameters in the growth model. Finally, we apply the method to actual size trajectory data constructed from the otolith ring measurements on delta smelt.

A STOCHASTIC MODEL OF INDIVIDUAL GROWTH

Model formulation

The individual growth model used in this paper is based on the energy flows shown in Fig. 1. Individual organisms encounter and ingest food, which is then assimilated. Assimilated food is transformed into reserve material such as protein and fat. A fixed fraction of the energy coming out of the reserve is used for both metabolic maintenance and growth, and the rest is used for reproduction. Translating the energy flow into a mathematical expression yields a system of differential equations with the size, or volume (V), of individuals and reserve density (E) as state variables (Table 1). The main biological assumptions are: (1) ingestion rate is proportional to the surface area ($V^{2/3}$) and related to food density through functional response ($f(t)$); (2) assimilation efficiency is constant; (3) the energy flux coming out of the reserve is determined so that the reserve density in a constant food environment is independent of individual size (reserve homeostasis; see Kooijman 2000: Section 3.4); (4) energy density within the reserve is regulated by a linear control process; (5) volume-specific cost of maintenance is constant; and (6) volume-specific cost for growth is constant. For additional assumptions and derivations of the growth model, readers are referred to Kooijman (2000) and Nisbet et al. (2000).

We assume that a fluctuating food supply ''drives'' the individual growth. Although there are other potential sources of variability in growth rate, we chose to incorporate the resource variability because it is one of the most important factors affecting growth rate. Many organisms, as they grow, have access to an increasing spectrum of food types and sizes and also may be more effective at catching them (Rose and Cowan 1993, Nobriga 2002). To describe this, we assume that a mean food level increases exponentially with the size of animals up to a certain critical size (V_c) and remains constant thereafter. Then we add a serially correlated signal to the mean food level such that the density of the food ($w(t)$) is given by Eq. 4 (Table 1). The independent random signal in the food density $z(t)$ is set to be a serially correlated Gaussian signal (pink noise; Nisbet and Gurney 2004). The coefficient $(S/\tau)^{1/2}$ in Eq. 5 (Table 1) maintains the variance of the signal unchanged with τ (see Muller and Nisbet 2000). The independent signal represents different environments (e.g., spatial resource heterogeneity) that are experienced by the individuals within a population. Finally, we use Holling's type II functional response ($f(t)$) to

link the food density and the ingestion rate (Eq. 3 in Table 1). A derivation of the functional response assuming a fixed handling time of food is presented in Kooijman (2000: Section 3.1.3).

The scaled functional response involves six parameters (w_h, α, β, V_c, S, and τ). However, w_h cannot be separated from α. This leaves five parameters (α, β, V_c, S, and τ) to be estimated. The first three parameters (α, β, and V_c) determine the ensemble average of food density that individuals of a given size experience, and the other two parameters (S and τ) determine the independent signal experienced among individuals. Throughout the paper, we assume that mean functional response is measured separately, and is thus known. This leaves the two free parameters (S and τ) in the food model to be estimated (Table 1).

Model characteristics

An important characteristic of the growth model is its inclusion of an energy reserve as a state variable. One key role of the reserve is the storage of energy in anticipation of periods of food shortage. Without such storage, organisms die unless they are able to feed without interruption. Thus the existence of the reserve is a ubiquitous feature of animals that inevitably experience a period without feeding. Fujiwara et al. (2004) have demonstrated that the reserve plays an important role in determining individual growth dynamics in a fluctuating food environment by acting as a low-pass filter that reduces variance and increases the temporal scale of autocorrelation in growth rate.

Inclusion of the reserve is also important for keeping track of energetic content within an individual. Fish and many other animals have limited ability to shrink their length, if shrinkage occurs at all. This is because the hard parts of the body (e.g., bones) prevent individuals from shrinking. Thus, without including the additional state variable that keeps track of the energy budget, which shrinks during starvation, a growth model becomes inconsistent with underlying energetic processes. Having an energy reserve and size as state variables in our model is analogous to having both mass and length in more detailed growth models (e.g., Gurney et al. 1990, Rose and Cowan 1993).

The model also has other desirable properties that are consistent with commonly observed growth dynamics of animals. For example, in a constant food environment (see Kooijman 2000: Section 3.7), the model reduces to a von Bertalanffy equation (von Bertalanffy 1938), which is often used to represent the individual growth of animals including fish (see Quinn and Deriso 1999: Section 4.2). On the other hand, when the available food increases with the size of animals, the model can exhibit accelerating growth with size. This is a frequently observed phenomenon of young fish in the field, and is often attributed to an increased availability of food due to increases in gape as well as the ability of fish to capture more food organisms

TABLE 1. Dynamic energy budget model.

a) Dynamics

Model equation	Equation no.
$\frac{dV(t)}{dt} = \frac{[\nu V^{2/3}E(t) - mgV(t)]_+}{g + E(t)}$	(1)
$\frac{dE(t)}{dt} = \frac{\nu}{V^{1/3}t}[f(t) - E(t)]$	(2)
$f(t) = \frac{w(t)}{w_h + w(t)}$	(3)
$w(t) = \begin{cases} \exp[\alpha + \beta V(t) + z(t)] & \text{when } V(t) < V_c \\ \exp[\alpha + \beta V_c + z(t)] & \text{when } V(t) > V_c \end{cases}$	(4)
$\frac{dz(t)}{dt} = \frac{-z(t)}{\tau} + \left(\frac{S}{\tau}\right)^{1/2}\eta(t)$	(5)

b) Variables and parameters

Term	Definition	Units
Unobservable variables		
$V(t)$	structural biovolume at time t; $V(t) = [\delta X(t)]^3$	mm^3
$E(t)$	scaled energy density in reserve at time t; actual energy density is $E_m E(t)$.	
$f(t)$	scaled functional response (Eq. 3)	
$z(t)$	a random signal that varies independently among individuals	
$\eta(t)$	a standard Gaussian signal	
Observable variables		
$X(t)$	length of individuals	mm
Parameters characterizing processes		
A_m	maximum assimilation rate per surface area	$J \cdot mm^{-2} \cdot d^{-1}$
M	maintenance energy per unit size per unit time	$J \cdot mm^{-3} \cdot d^{-1}$
G	energy costs for a unit increase in size	J/mm^3
E_m	maximum reserve density	J/mm^3
w_h	a half-saturation constant in the functional response	
Parameters for which crude estimates are available from separate information		
δ	shape correction factor (see Kooijman 2000: Sec. 8.2)	
κ	fraction of utilized energy spent on maintenance and growth	
V_c	size of organisms at which food density becomes independent of the size	
α, β	slope and intercept parameters associated with food	
Parameter combinations that we hope to estimate		
m	maintenance rate coefficient, $m = \frac{M}{G}$	d^{-1}
ν	energy conductance rate, $\nu = \frac{A_m}{E_m}$	mm/d
g	energy investment ratio, $g = \frac{G}{\kappa E_m}$	
τ	memory retention time of the food signal	
S	variance of the food signal	

Note: This table was adapted from Nisbet et al. (2000: Table 2). In model 1, the subscript + indicates that the quantity in parentheses must be nonnegative.

(Ricker 1958). Furthermore, a stochastic version of the model (Fujiwara et al. 2004) exhibits increasing variance of size among individuals with age (growth depensation), followed by decreased variance of size (growth compensation), which are also phenomena often observed in the growth of fish and other animals (Ricker 1958, DeAngelis and Huston 1987).

Finally, the growth model is expressed with two state equations, one functional response and a small number of parameters. Simulating this model is straightforward based on the Ito interpretation of stochastic differential equations (Higham 2001).

Parameter Estimation by Nonlinear State–Space Method

Our goal is to estimate two free parameters from size trajectory data. The growth model has two state equations with three free parameters (v, m, and g) that determine physiological rates within individuals, together with one equation determining food variability, which contains two additional free parameters (S and τ) that need to be estimated (Table 1).

Fitting the individual growth model to size trajectories is complicated by the inclusion of an unobservable state variable (reserve density, $E(t)$). Here, we use the nonlinear state–space method, which accommodates the ''hidden'' state variable, in order to fit the model to the data. In this method, the size of an individual is forecasted numerically based on its previous sizes and initial reserve density. Using the forecasted size distribution, a likelihood is calculated. Finally, best-fit parameter values that maximize the likelihood are searched for. A similar method has been applied to estimate parameters in population models (deValpine and Hastings 2001). Here, we describe the algorithm pictorially and also provide MATLAB (Version 6.1; MathWorks 2001) code as an example in the supplement. More mathematically rigorous presentation for particle filtering can be found in Doucet et al. (2001) and de Valpine (2004).

The size trajectory data consist of size x_{it} of individual i ($i = 1, \ldots, N$) at age t ($t = 0, \ldots, T_i$) from the time of the first size measurement of the individual, where N is the number of individuals in the sample and T_i is the final age at which the size of individual i is determined. At age 0, we know the actual size of the individual (x_{i0}), and know or assume the value of the functional response. Furthermore, we set the expected reserve density to $E_0 = f_0$, which is the expected value when the scaled functional response $f(t) = f_0$. Let $l_{i,t}$ (v, m, g, S, τ) be the likelihood associated with the sizes of a single individual i at age t ($1 < t \leq T_i$) that is conditional on all previous sizes of the individual, which is then calculated for individual i using the following recursive algorithm:

1. *Projection from age 0 to 1*.—The size at age 1 is projected 3000 times using the initial conditions, the equations in Table 1, and a given set of parameter values (Fig. 2a). The projected sizes are either equal to or greater than x_{i0} because the model does not allow shrinkage. Let c_{i1} be the number of projected sizes that are equal to x_{i0} (i.e., no growth). Then $p_{i1} = c_{i1}/3000$ gives the probability of no growth, and $1 - p_{i1}$ gives the probability of positive growth. A probability density of the size of the individual i at age t conditional on positive growth and the size at age 0 ($\Pr(x_{i1} | x_{i1} > x_{i0}, x_{i0})$; Fig. 2c) is calculated by smoothing the histogram of projected sizes (Fig. 2b).

2. *Likelihood at age 1*.—The likelihood associated with the observed size at age $t = 1$ of individual i is given by the following:

$$l_{i1}(v, m, g, S, \tau) = \begin{cases} p_{i1} & \text{when } x_{i1} = x_{i0} \\ (1 - p_{i1})\Pr(x_{i1} | x_{i1} > x_{i0}, x_{i0}) & \text{when } x_{i1} > x_{i0}. \end{cases}$$

3. *Filtering at age 1*.—At age 1, each projected size also has an underlying projected reserve density (Fig. 2d) and food, which led to the size and reserve density. Because we know the actual size of the individuals at age 1, we take the projected sizes that are ''close'' to the actual size (horizontal band in Fig. 2d), along with the associated reserve density (Fig. 4e) and food trajectory. Simulations suggest that defining ''close'' to be ''within 0.15 times the standard deviation of size at age in the data'' is a good rule of thumb (i.e., it balances the number of trajectories that pass through the width and that are filtered out; see de Valpine [2004] for other ways of selecting the width). Then the sets of the projected sizes, reserve density, and food level at age 1 are sampled with replacement 3000 times.

4. *Projection from age 1 to 2*.—We now have 3000 sets of projected size, reserve density, and food trajectory. From each of the sets, the size at age 2 is projected using the individual growth equations (Table 1) and the same set of parameter values used at age 1 (Fig. 2f). From the number of projected sizes that are equal to x_{i1}, the probability of no growth (p_{i2}) and conditional probability density $\Pr(x_{i2} | x_{i2} > x_{i1}, x_{i1}, x_{i0})$ are calculated.

5. *Likelihood at age 2*.—Again, projected sizes are either equal to or greater than x_{i1}. The likelihood associated with age $t = 2$ of individual i is given by:

$$l_{i2}(v, m, g, S, \tau) = \begin{cases} p_{i2} & \text{when } x_{i2} = x_{i1} \\ (1 - p_{i2})\Pr(x_{i2} | x_{i2} > x_{i1}, x_{i1}, x_{i0}) & \text{when } x_{i2} > x_{i1}. \end{cases}$$

6. *Filtering at age $t - 1$*.—In general, at age $t - 1$ ($2 < t \leq T_i$), projected sets of size, reserve density, and food trajectories are selected based on the actual size of individuals as in step 3. Then the sets are sampled with replacement 3000 times.

7. *Projection from age $t - 1$ to t (for $t > 2$)*.—From each of the sampled sets, the size at age t is projected

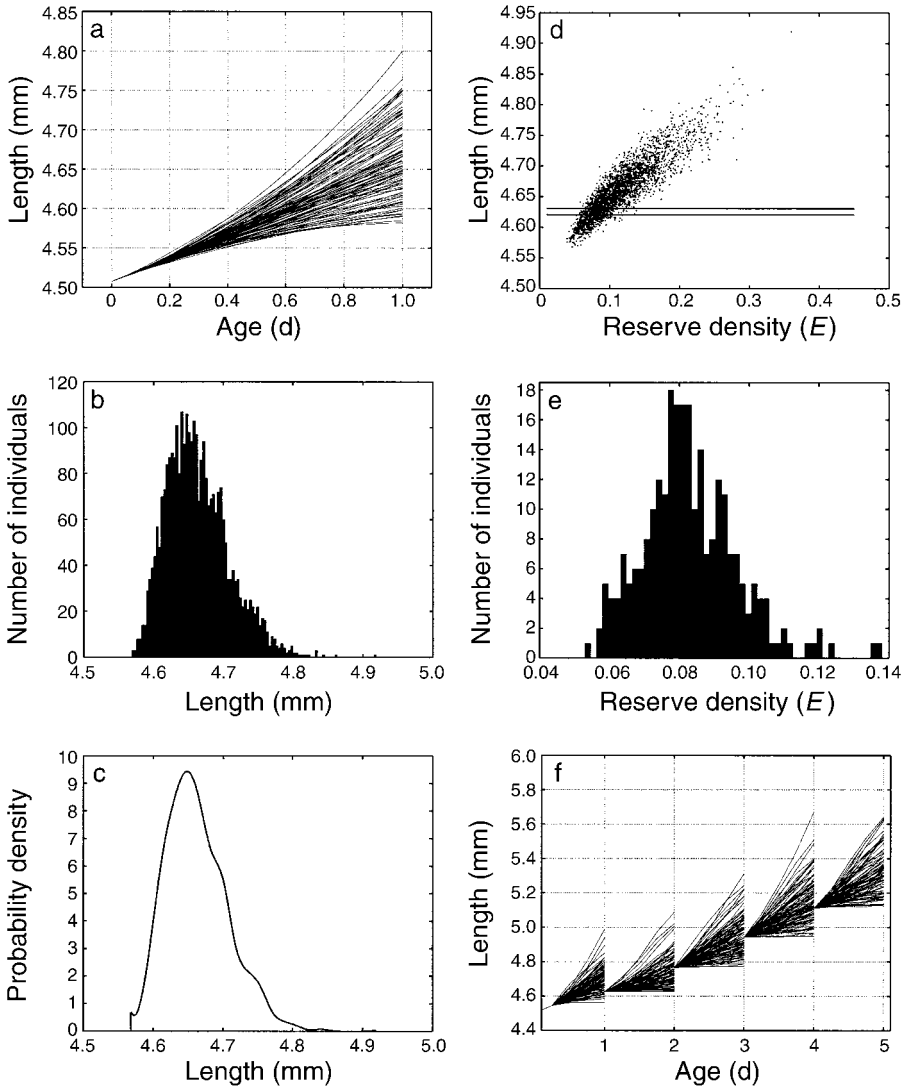

FIG. 2. Parameter estimation algorithm. (a) Projected length of individuals from age 0 to 1 for individual i; 100 out of 3000 trajectories are plotted. (b) Histogram of simulated length at age $t = 1$ for individual i. (c) Probability density function of length at age 1 approximated by applying a cubic spline to the histogram. (d) Scatter plot of simulated reserve density and length at age $t = 1$ for individual i. (e) Histogram of projected reserve density for individual i at age $t = 1$ after filtering process [i.e., individuals within the two lines in (d)]. Individuals within the two lines in (d) were sampled with replacement 3000 times to be used for projecting the size of the individual at age $t = 2$. (f) Projections of size from age 0 to 5 for an individual. They are filtered at ages 1, 2, 3, and 4 at the known lengths of the individual; 100 of 3000 trajectories are plotted.

using equations in Table 1 and the same set of parameter values used previously (Fig. 2f).

8. *Likelihood at age t (for $t > 2$).*—At age t, the likelihood is calculated from the probability of no growth and the fitted density function to projected sizes in the same way it was done at ages $t = 1$ and 2:

$$l_{i,t}(\nu, m, g, S, \tau) = \begin{cases} p_{i,t} & \text{when } x_{i,t} = x_{i,t-1} \\ (1 - p_{i,t})\Pr(x_{i,t} \mid x_{i,t-1} > x_{i1}, x_{i,t-1}, \ldots, x_{i0}) & \text{when } x_{i,t} > x_{i,t-1}. \end{cases}$$

9. *Sequential likelihood integrals.*—Steps 6–8 are repeated until $t = T_i$ in order to obtain the likelihoods associated with the sizes of individual from $t = 1$ to T_i:

$$[l_{i1}(\nu, m, g, S, \tau), l_{i2}(\nu, m, g, S, \tau), \ldots, l_{iT}(\nu, m, g, S, \tau)].$$

We emphasize that the likelihood here is conditional on all previous sizes. This is repeated for all individuals ($i = 1, \ldots, N$). Because we assume that the noise experienced by individuals is independent, the log likelihood associated with the trajectory data of all N individuals evaluated at the set of parameter values is given by the following:

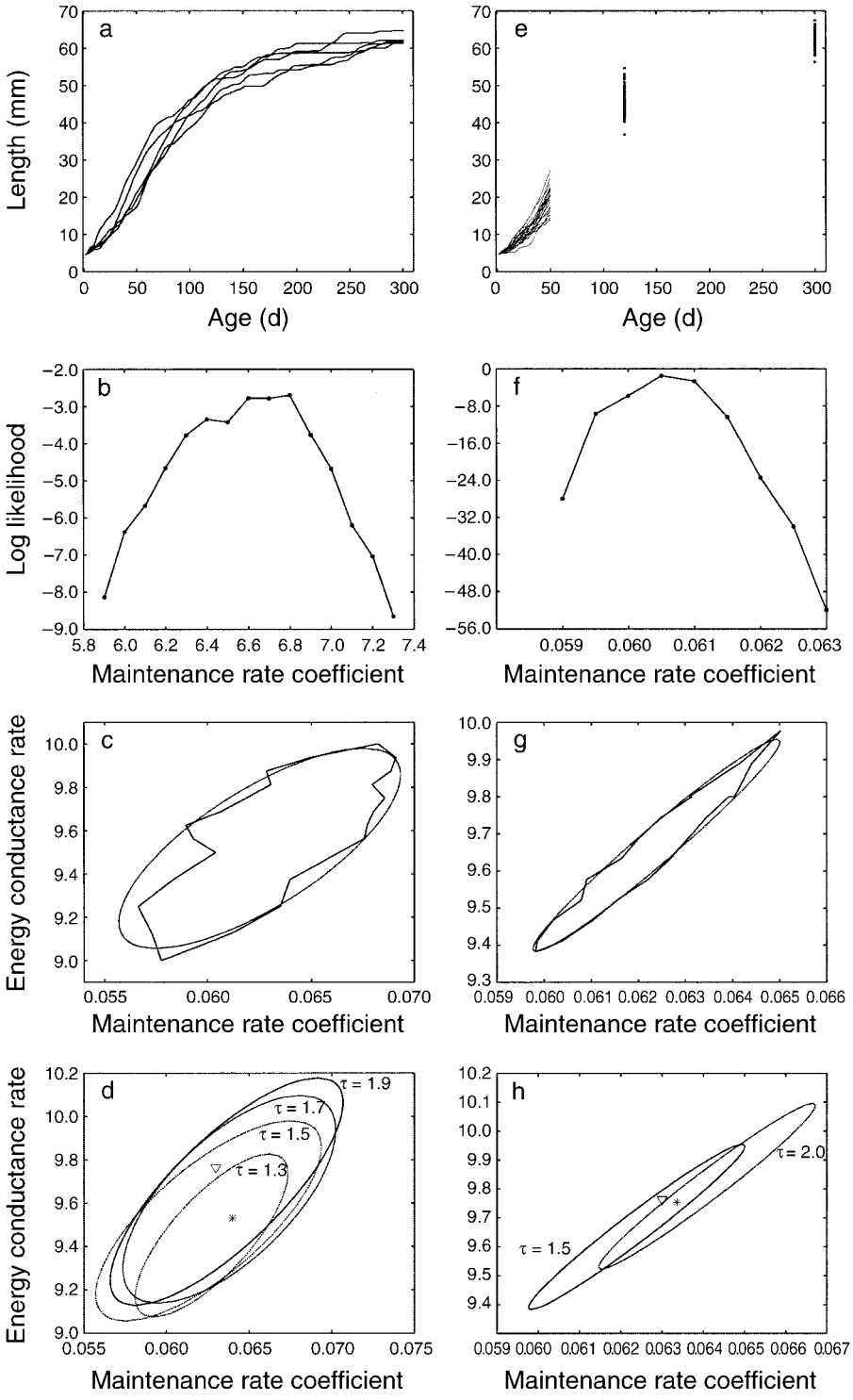

FIG. 3. Determination of estimability of parameters. (a) Simulated single-trajectory data: one size trajectory measured daily from age 0 to 300. (b) Profile log likelihood (the difference from the maximum-likelihood value over m, ν, and τ when $S = 1.0$) of maintenance rate coefficient (m) when $\nu = 9.875$, $\tau = 1.5$, and $S = 1.0$. (c) Estimated 95% confidence region (solid) of energy conductance rate (ν) and maintenance rate coefficient (m) when memory retention time of the food signal $\tau = 1.5$ and variance of the food signal $S = 1.0$ (df = 3). An ellipse (dotted line) was fitted visually to the confidence region. (d) Estimated 95% confidence region (visually fitted ellipses) at $\tau = 1.3$, 1.5, 1.7, and 1.9. Panel (d) also shows true values (triangle when $\tau = 1.5$) and the maximum-likelihood estimate (star when $\tau = 1.6$). (e) Simulated size distribution data: 20 individual size trajectories measured daily from ages 0 to 50 and 100 individual size distributions at ages 120 and 300. Parameters used to simulate the data are $\nu = 9.7639$, $m = 0.063$, $\tau = 1.5$, $S = 1.0$, and $g = 1.286$ (where g is the

TABLE 2. Maximum-likelihood estimates and the difference in maximum log likelihood using the single-trajectory data.

Scenario	ν	m	g	S	τ	Δ log likelihood
True values	9.8	0.063	1.2	1.0	1.5	
1	9.4	0.063	(1.29)	(1.0)	1.6	0
2	8.7	0.058	(1.29)	(5.0)	4.7	−21
3	15.2	0.112	(1.29)	(0.2)	2.8	−18
4	9.5	0.062	(1.29)	(1.0)	(1.5)	−2
5	13.8	0.040	(3.00)	(1.0)	(1.5)	−6

Notes: The second row shows the true parameters used to simulate the data. In the rows above, the parameters in parentheses were fixed as constants, and the log likelihood was maximized over other parameters. The difference in log likelihood is measured from the maximum-likelihood value under Scenario 1. We used $\alpha = 0.137$, $\beta = 2.75$, $V_c = 800$ in Eq. 4 and $\delta = 1$ in Table 1.

$$L(\nu, m, g, S, \tau) = \sum_i \sum_t \log[l_{i,t}(\nu, m, g, S, \tau)]. \quad (6)$$

Finally, a set of parameters that maximizes the log likelihood function is the maximum-likelihood estimate of the parameters.

We note a caveat with the nonlinear state–space method. Because the probability density is constructed using simulation of a stochastic model, there is an error associated with it. Consequently, when likelihood is evaluated repeatedly at the same parameter values, they differ slightly but non-negligibly (i.e., likelihood is stochastic; see Doucet et al. 2001). To overcome this problem, we estimated the likelihood with the same set of parameter values multiple times in order to obtain a convergence. For example, we evaluated the likelihood eight times at the same parameter values in the current analysis. This stochasticity increases with the number of $l_{i,t}(\cdot)$) evaluations in Eq. 6, and thus increases with the size of the data. Although the confidence interval associated with each parameter will shrink with the size of the data, the numerical error will increase with the data. However, this problem should be overcome by increasing the number of simulations in evaluating the probability density (i.e., by increased speed of computers).

ESTIMABILITY OF PARAMETERS IN A DYNAMIC ENERGY BUDGET MODEL

To demonstrate the estimability of parameters, we fitted the model to two types of simulated data sets. These data sets are motivated by the actual data available for delta smelt. In one data set, a size trajectory of a single individual over 300 days is used (Fig. 3a); we call this single-trajectory data. In the other data set, size trajectories of 20 individuals over 50 days, as well as size distributions of 100 individuals at time $t = 120$ and 300, are used (Fig. 3e). The sizes of individuals at time $t = 120$ in the latter data set were treated as independent trajectories, each consisting of two points (a typical size at birth and a size at $t = 120$). We treated the sizes at $t = 300$ in the same way. We call this data set size ''distribution data.'' In these examples, we used the term ''length'' as a cubic root of the volume and assumed that the initial length of the individuals was known to be 4.5 mm. The values used for parameters are shown in Table 2.

Parameters are estimable using a maximum-likelihood method when they are not confounded in a likelihood function. They may be confounded because there is not enough variation in the data (extrinsic estimability problem), or because different parameters specify the same variation in the data (intrinsic estimability problem; see McCullagh and Nelder 1989). Here, we are addressing estimability of parameters from specific types of data and a model. Thus, we are taking a practical approach without separating these causes. When an analytical expression for a likelihood function is available, estimability of parameters can be determined from second derivatives of the likelihood function with respect to the parameters (see Catchpole and Morgan 1997). Because we do not have the analytical expression, we examine likelihood values near its maximum to examine the estimability. We consider that, if the likelihood is peaked at a unique set of parameter values, then the parameters are estimable. In order to do this, we first found the maximum-likelihood value and compared it with likelihoods over the pa-

←

energy investment ratio). (f) Profile log likelihood (the difference from the maximum-likelihood value over m, ν, and τ when $S = 1.0$) of maintenance rate coefficient (m) when $\nu = 9.400$, $\tau = 1.5$, and $S = 1.0$. (g) Estimated 95% confidence region (solid) of energy conductance rate (ν) and maintenance rate coefficient (m) when $\tau = 1.5$, and $S = 1.0$ (df = 3). An ellipse (dotted line) was fitted visually to the confidence region. (h) Estimated 95% confidence region (visually fitted ellipses) at $\tau = 1.5$ and 2.0. Panel (h) also shows true values (triangle when $\tau = 1.5$) and the maximum-likelihood estimate (star when $\tau = 1.8$).

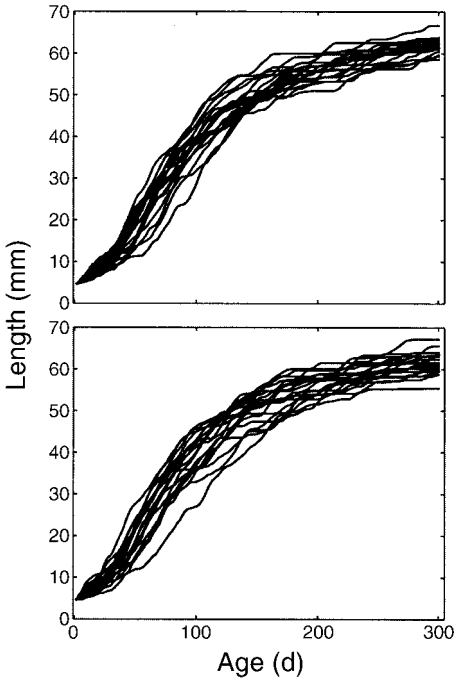

FIG. 4. Simulated size trajectories using estimated parameters: (a) maximum-likelihood estimates ($\hat{\nu} = 9.4$, $\hat{m} = 0.063$, $\hat{\tau} = 1.6$) based on the single-trajectory data in Fig. 3a; (b) maximum-likelihood estimates ($\hat{\nu} = 9.8$, $\hat{m} = 0.063$, $\hat{\tau} = 1.8$) based on the size distribution data in Fig. 3e. For both figures, 20 simulated size trajectories are shown.

rameter space around the maximum-likelihood estimates.

For both data types, we evaluated likelihood at various values of m while other parameters were fixed as constant, producing a projection of profile likelihood over m (Fig. 3b, f). This likelihood was then repeated at different values of ν while the rest of the parameters were fixed as constant, producing profile likelihood projections over ν and m (Fig. 3c, g). The maximum values of the likelihood in Fig. 3c and g were taken as conditional maximum-likelihood values (conditional on the other parameters). The whole process was repeated over various values of τ to search for a maximum-likelihood value over the three parameters (Fig. 3d, h). With both data types, the maximum-likelihood value peaked at a unique set of parameter values, indicating that the three parameters are estimable. Based on these parameters, size trajectories were simulated (Fig. 4).

Using the single-trajectory data, we searched for maximum-likelihood values over the three parameters (ν, m, and τ) at three different values of S ($S = 0.2$, 1.0, and 5.0; Scenarios 1, 2, and 3 in Table 2). The maximum-likelihood values were different at different values of S, indicating that the likelihood is maximized at a unique set of parameter values over the four parameters (ν, m, τ, and S). Thus, at least the four parameters (ν, m, τ, and S) are estimable separately. Similarly, the likelihood was maximized over ν and m at two different values of g ($g = 1.0$ and 3.0), while the rest of the parameters were fixed as constant (Scenarios 4 and 5 in Table 2). The maximum-likelihood values were different at different values of g, indicating that g is also estimable when we know S and τ from separate information.

Fitting the model to simulated data sets revealed the covariance structure of parameters. For example, ν and m are positively correlated with each other. This is consistent with the fact that the ratio ν/m determines the maximum size of individuals when $f(t)$ is a constant (Kooijman 2000: Section 3.7). We also found that S and m (thus, also S and ν) are negatively correlated with each other. This reflects the fact that when the mean functional response is below 0.5, as in our examples during the early part of the life stage, the mean functional response is increased with S because of the form of nonlinearity in the functional response (the Holling's type II). The increased mean functional response is compensated by the reduced m, which determines how quickly an individual reaches the maximum size.

DELTA SMELT SIZE TRAJECTORY ANALYSIS

The delta smelt (*Hypomesus transpacificus*) is a euryhaline fish that is endemic to San Francisco Estuary, California, USA (Moyle et al. 1992, Sweetnam 1999; W. A. Bennett, *unpublished manuscript*). It generally has an annual life span and spawns from March to June (W. A. Bennett, *unpublished manuscript*). Its population size declined dramatically during the early 1980s, prompting its listing as a federal and state threatened species (U.S. Department of Interior 1994). The cause of the decline is yet to be determined, but is thought to have occurred due to dramatic changes in the estuarine food web from non-native invasive species, losses in freshwater exported from the estuary by the federal and state water pumping projects, as well as the effects of toxicants such as pesticides (Bennett and Moyle 1996; W. A. Bennett, *unpublished manuscript*).

Delta smelt used for the longitudinal size at age estimates using otoliths were collected in the estuarine low-salinity zone in collaboration with monitoring of summer juvenile fish conducted by the Interagency Ecological Program for the San Francisco Estuary. Delta smelt were sampled using a plankton net attached to a towing sled, measured, and then fixed in 70% ETOH. Detailed methods on otolith preparation and analysis are presented in Hobbs et al. (2004). Briefly, sagittal otoliths were extracted, mounted on slides, and polished. Ring microstructure was then evaluated using a light microscope attached to a computer with image analysis software (Image Pro 4; MediaCybernetics 1998).

We used individual size trajectories of five individuals that lived longer than 170 days (Fig. 5a), and fitted the model to the data. Because the shape of the fish is

not a cube, we used a shape correction factor (δ = 0.238; Table 2) estimated by Kooijman (2000: Section 8.2) for sand smelt (*Atherina presbyter*). In our analysis, we set values of α and β in Eq. 4 so that $\bar{f}(0) = 0.1$ at birth and $\bar{f}(t) = 0.5$ when $V(t) = V_c$. The lower bound of the average food density was chosen so that it is small but still provides room for fluctuations, and the upper bound was set so that it allows some individuals to grow in fluctuating environments up to twice the size of individuals in average food environments. We also set $V_c = 800$ mm^3, which is approximately the inflection point of the growth curves, and $g = 1$, which is a very crude estimate. We note that, in reality, these values have associated uncertainties. Because our goal of this paper is to demonstrate a statistical method, we assume that there is no uncertainty associated with them. Consequently, the actual estimates of other parameters should be interpreted cautiously.

The maximum-likelihood estimates of the four parameters (and associated standard errors) are $\hat{\nu} = 3.25$ (0.02) mm/d, $\hat{m} = 0.109$ (0.01)/d, $\hat{\tau} = 0.46$ (0.002) d, and $\hat{S} = 1.81$ (0.02). Based on these estimates, size trajectories were simulated (Fig. 5b).

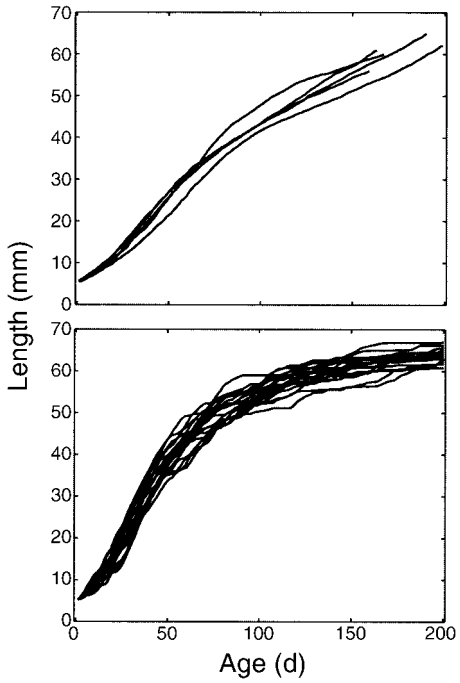

FIG. 5. Delta smelt (*Hypomesus transpacificus*) size trajectories: (a) actual size trajectory data of five individuals and (b) 20 simulated trajectories based on maximum-likelihood estimates ($\hat{\nu} = 3.2$, $\hat{m} = 0.11$, $\hat{\tau} = 0.5$, and $\hat{S} = 1.8$).

DISCUSSION

The numerical maximum-likelihood approach outlined in this paper allows estimation of parameters in a system of nonlinear stochastic differential equations in which one of the state variables is unobservable. We used this method to estimate parameters in an energetic-based individual growth model (a dynamic energy budget model) from size trajectory data.

The advantage of obtaining parameters in a mechanistic model such as the one used in this paper is that results can be interpreted in relation to physiological rate processes that can be measured independently. For example, our estimated maintenance rate coefficient for delta smelt is 0.11 d^{-1}. According to dynamic energy budget theory, the respiration rate of a growing organism is the sum of maintenance rate and the overheads associated with growth (Kooijman 2000, Nisbet et al. 2000). Our fit thus implies that a delta smelt will respire at a rate equivalent to not less than 11% of its body mass per day.

We investigated estimability of parameters in dynamic energy budget models. This is an important step in developing a new likelihood-based parameter estimation method, because some parameters may be inestimable, and extra information must be provided to estimate them (e.g., Fujiwara and Caswell 2001). We found that the maintenance rate coefficient (m), energy conductance rate (ν), variance in food (S), and memory retention time in food (τ) can be estimated separately if we know the energy investment ratio (g) and the mean functional response level. This scenario was applied to the analysis of growth in delta smelt. Alternatively, if we know how food fluctuates over time and how individual feeding rate responds to it, we can estimate all three parameters (m, ν, and g) associated with the individual growth model. This also emphasizes the importance of obtaining accurate food conditions of organisms along with size trajectories.

The fact that g is separable from ν is counterintuitive because the two parameters only appear as ν/g in a deterministic model. We hypothesize that the information on g in the data comes from the autocorrelation in the size trajectory. Therefore, g, ν, and τ are unlikely to be estimable together.

The parameter estimation technique presented here is an application of the method commonly called state–space model analysis and has been useful in separating variability in different processes (e.g., de Valpine and Hastings 2001). In this paper, we assumed that variability in growth rates originates from the fluctuation in available food. Other potential sources of the variability include measurement noise and difference in growth parameters among individuals and over time. For example, the difference among individuals could be environmentally determined during the early life of individuals, or it could be genetically determined. The parameters could vary over time due to variable toxic effects. The state–space analysis method provides a potential tool to separate these different types of signals originating from the different processes.

Comparing actual (Fig. 5a) and fitted (Fig. 5b) trajectories of delta smelt suggests the potential need for improvements in the growth and/or food model. For

example, model trajectories grow more rapidly and asymptote more quickly than actual trajectories. This might be overcome with the inclusion of other factors such as temperature change, and more accurate representation of food availability in the model or improvement in the energy allocation rule. Furthermore, model size trajectories have more day-to-day variability than the data, as evidenced by more ''wiggliness'' associated with lines in Fig. 5b than in Fig. 5a. This suggests an inflated estimate of S in Eq. 5. We could separate variation within and between individuals by including individual heterogeneity in growth parameters.

One important factor influencing the growth of individuals is availability of food, and we made one special assumption relating food availability to organism size. We expect variability among populations with regard to how the food availability changes throughout the life history of individuals, reflecting differences in the community structures in which those individuals live. One way to accommodate such variability is to incorporate extensive information on food organisms into the model. For example, Rose and Cowan (1993) used measured changes in the distribution of various food organisms, known size-specific behavior of fish, and other environmental factors such as the length of daylight period and temperature to model how the availability of food for striped bass (*Morone saxatilis*) changes with size and the day of the year. When such data on food and feeding are available, they can be used as covariate data specifying the food density in the growth model.

The parameter estimation method outlined in this paper is based on likelihood theory. Therefore, model selection criteria such as Akaike Information Criteria (AIC; Burnham and Anderson 1997) can be applied to select best-fit models. In this paper, we only used one type of model. However, a variety of energetic-based individual growth models exists (e.g., Noonburg et al. 1998). Comparison of the models using AIC or other model selection methods would be an interesting future project.

We note that the parameters estimated in this paper are ones for surviving individuals. Therefore, careful interpretation of the results is needed when size-dependent mortality is severe. We are currently investigating the feasibility of including size-dependent mortality in the parameter estimation method.

Individual growth rate of animals is increasingly used as an ecological indicator (e.g., Bennett et al. 1995). Stresses, such as contaminants in the environment, often affect energetic processes within individuals, which, in turn, affect individual growth rate. Thus it is important to be able to estimate parameters in energetic-based individual growth models. The method presented in this paper uses longitudinal individual size data, in which the size of the same individuals is measured repeatedly over time, to estimate parameters in the growth models. The collection of size trajectory data is becoming increasingly more common. It can be conducted in vivo by repeatedly measuring the size of marked individuals, and can be reconstructed retrospectively from patterns in hard body parts such as otolith rings and shells. Thus we expect this technique to become an important tool in ecological research.

Acknowledgments

We thank Jim Hobbs for supplying the delta smelt otolith data and André M. de Roos, Perry de Valpine, and Lewi Stone for constructive comments and suggestions. This research has been supported by a grant from the U.S. Environmental Protection Agency's Science to Achieve Results (STAR) Estuarine and Great Lakes (EaGLe) program through funding to the Pacific Estuarine Ecosystem Indicator Research (PEEIR) Consortium, U.S. EPA Agreement #R-882867601.

Literature Cited

Bennett, W. A., and P. B. Moyle. 1996. Where have all the fishes gone? Factors producing fish declines in the San Francisco Bay estuary. Pages 519–541 *in* J. T. Hollibaugh, editor. San Francisco Bay: the ecosystem. Pacific Division, American Association for the Advancement of Science, San Francisco, California, USA.

Bennett, W. A., D. J. Ostrach, and D. E. Hinton. 1995. Condition of larval striped bass in a drought-stricken estuary: evaluating pelagic food web limitation. Ecological Applications **5**:680–692.

Burnham, K. P., and D. R. Anderson. 1997. Model selection and inference: a practical information-theoretic approach. Springer-Verlag, New York, New York, USA.

Campana, S. E., and J. D. Neilson. 1985. Microstructure of fish otoliths. Canadian Journal of Fisheries and Aquatic Sciences **42**:1014–1032.

Caswell, H. 2001. Matrix population models: construction, analysis and interpretation. Second edition. Sinauer Associates, Sunderland, Massachusetts, USA.

Catchpole, E., and B. Morgan. 1997. Detecting parameter redundancy. Biometrika **84**:187–196.

Cox, D. K., and C. C. Coutant. 1981. Growth dynamics of juvenile striped bass as functions of temperature and ration. Transactions of the American Fisheries Society **110**:226–238.

DeAngelis, D. L., and M. A. Huston. 1987. Effects of growth rates in models of size distribution formation in plants and animals. Ecological Modelling **36**:119–137.

DeAngelis, D. L., L. B. Rose, E. A. Crowder, E. A. Marshall, and D. Lika. 1993. Fish cohort dynamics: application of complementary modeling approaches. American Naturalist **142**:604–622.

de Valpine, P. 2004. Monte Carlo state–space likelihoods by weighted posterior kernel density estimation. Journal of the American Statistical Association **99**:523–536.

de Valpine, P., and A. Hastings. 2001. Fitting population models incorporating process noise and observation error. Ecological Monographs **72**:57–76.

Diggle, P. J., P. Heagerty, K. Y. Liang, and S. L. Zeger. 2002. Analysis of longitudinal data. Second edition. Oxford Statistical Science Series 25. Oxford University Press, Oxford, UK.

Doucet, A., N. de Freitas, and N. J. Gordon. 2001. Sequential Monte Carlo methods in practice. Springer-Verlag, New York, New York, USA.

Fujiwara, M., and H. Caswell. 2001. A general approach to temporary emigration in mark–recapture analysis. Ecology **83**:3266–3275.

Fujiwara, M., B. E. Kendall, and R. M. Nisbet. 2004. Growth autocorrelation and animal size variation. Ecology Letters **7**:106–113.

Gordon, N. J., D. J. Salmond, and A. F. M. Smith. 1993. Novel-approach to nonlinear non-Gaussian Bayesian state estimation. IEE (Institute of Electrical Engineers) Proceedings, F Radar and Signal Processing **140**:107–113.

Gurney, W. S. C., W. Jones, A. R. Veitch, and R. M. Nisbet. 2003. Resource allocation, hyperphagia, and compensator growth in juveniles. Ecology **84**:2777–2787.

Gurney, W. S. C., E. McCauley, R. M. Nisbet, and W. W. Murdoch. 1990. The physiological ecology of daphnia: a dynamic-model of growth and reproduction. Ecology **71**: 716–732.

Higham, D. J. 2001. An algorithmic introduction to numerical simulation of stochastic differential equations. Society for Industrial and Applied Mathematics SIAM Review **43**:525–546.

Hobbs, J. A., W. A. Bennett, J. E. Burton, and B. Baskerville-Bridges. 2004. Age and growth validation of delta smelt (*Hypomesus transpacificus*) in the San Francisco Estuary. Dissertation. University of California, Davis, California, USA.

Kooijman, S. A. L. M. 1986. Population dynamics on the basis of budgets. *In* J. A. J. Metz and O. Diekmann, editors. The dynamics of physiologically structured populations. Springer Lecture Notes in Biomathematics. Springer-Verlag, Berlin, Germany.

Kooijman, S. A. L. M. 2000. Dynamic energy and mass budgets in biological systems. Second edition. Cambridge University Press, Cambridge, UK.

Kooijman, S. A. L. M., and J. J. M. Bedaux. 1996. The analysis of aquatic toxicity data. VU (Vrije Universiteit) University Press, Amsterdam, The Netherlands.

MathWorks. 2001. MATLAB. Version 6.1, release 12. MathWorks, Natick, Massachusetts, USA.

McCullagh, P., and J. A. Nelder. 1989. Generalized linear models. Monographs on statistics and applied probability 37. Second edition. CRC Press, Boca Raton, Florida, USA.

MediaCybernetics. 1998. Image-Pro Plus. Version 4. Media Cybernetics, Silver Spring, Maryland, USA.

Moyle, P. B., B. Herbold, D. E. Stevens, and L. W. Miller. 1992. Life history and status of delta smelt in the Sacramento–San Joaquin estuary, California. Transactions of the American Fisheries Society **121**:67–77.

Muller, E. B., and R. M. Nisbet. 2000. Survival and production in variable resource environments. Bulletin of Mathematical Biology **62**:1163–1189.

Nisbet, R. M., and W. S. C. Gurney. 2004. Modeling flauctuating populations. Blackburn Press, Caldwell, New Jersey, USA.

Nisbet, R. M., E. McCauley, W. S. C. Gurney, W. W. Murdoch, and S. N. Wood. 2004. Formulating and testing a dynamic energy budget model. Ecology **85**:3132–3139.

Nisbet, R. M., E. B. Muller, K. Lika, and S. A. L. M. Kooijman. 2000. From molecules to ecosystems through dynamic energy budget models. Journal of Animal Ecology **69**:913–926.

Nobriga, M. 2002. Larval delta smelt diet composition and feeding incidence: environmental and ontogenetic influences. California Fish and Game **88**(4):149–164.

Noonburg, E. G., R. M. Nisbet, E. McCauley, W. S. C. Gurney, W. W. Murdoch, and A. M. De Roos. 1998. Experimental testing of dynamic energy budget models. Functional Ecology **12**:211–222.

Pfister, C. A., and S. D. Peacor. 2003. Variable performance of individuals: the role of population density and endogenously formed landscape heterogeneity. Journal of Animal Ecology **72**:725–735.

Pfister, C. A., and F. R. Stevens. 2002. Genesis of size variability in plants and animals. Ecology **83**:59–72.

Quinn, T. J.,II, and R. B. Deriso. 1999. Quantitative fish dynamics. Oxford University Press, Oxford, UK.

Rice, J. A., T. J. Miller, K. A. Rose, L. B. Crowder, E. A. Marschall, A. S. Trebitz, and D. L. DeAngelis. 1993. Growth-rate variation and larval survival—inferences from an individual-based size-dependent predation model. Canadian Journal of Fisheries and Aquatic Sciences **50**:133–142.

Ricker, W. E. 1958. Handbook of computations for biological statistics of fish populations. The Fisheries Research Board of Canada, Ottawa, Canada.

Rogers, B. A., and D. T. Westin. 1981. Laboratory studies on effects of temperature and delayed initial feeding on development of striped bass larvae. Transactions of the American Fisheries Society **110**:100–110.

Rose, K. A., and J. H. Cowan. 1993. Individual-based model of young-of-the-year striped bass population dynamics. I. Model description and baseline simulations. Transactions of the American Fisheries Society **122**:415–438.

Sweetnam, D. A. 1999. Status of delta smelt in the Sacramento–San Joaquin Estuary. California Fish and Game **85**: 22–27.

U.S. Department of Interior. 1994. Endangered and threatened wildlife and plants: critical habitat determination for delta smelt. U.S. Fish and Wildlife Service, Washington, D.C., USA. Federal Register Document 94-31063.

van Haren, R. J. F., and S. A. L. M. Kooijman. 1993. Application of a dynamic energy budget model to *Mytilus edulis* (L.). Netherlands Journal of Sea Research **31**(2): 119–133.

von Bertalanffy, L. 1938. A quantitative theory of organic growth (inquiries on growth laws II). Human Biology **10**(2):181–213.

Wikelski, M., V. Carrillo, and F. Trillmich. 1997. Energy limits to body size in a grazing reptile, the Galapagos marine iguana. Ecology **78**:2204–2217.

SUPPLEMENT

Matlab source code for the algorithm described in our study is available in ESA's Electronic Data Archive: *Ecological Archives* E086-079-S1.